

Dip Coating Passivation of Crystalline Silicon by Lewis Acids

Wenbo Ji^{1,2,3}, Yingbo Zhao^{1,2}, Hossain M. Fahad^{1,2}, James Bullock^{1,2}, Thomas Allen⁴, Der-Hsien Lien^{1,2}, Stefaan De Wolf⁴, Ali Javey^{1,2,}*

¹ Electrical Engineering and Computer Sciences, University of California, Berkeley, California 94720, USA

² Materials Sciences Division, Lawrence Berkeley National Laboratory, Berkeley, California 94720, USA

³ Materials Science and Engineering, University of California, Berkeley, California 94720, USA

⁴ KAUST Solar Center (KSC), King Abdullah University of Science and Technology (KAUST), Thuwal 23955-6900, Saudi Arabia

KEYWORDS: Lewis acids, Nafion, crystalline silicon, room-temperature passivation, charge transfer

ABSTRACT: The reduction of carrier recombination processes by surface passivation is vital for highly efficient crystalline silicon (c-Si) solar cells and bulk wafer metrological characterization. Herein, we report a dip coating passivation of silicon surfaces in ambient air and temperature with Nafion, achieving a champion effective carrier lifetime of 12 milliseconds on high resistivity *n*-type c-Si, which is comparable to state-of-the-art passivation methods. Nafion is a non-reactive polymer with strong Lewis acidity, thus leading to the formation of a large density of fixed charges at silicon surface; 1-2 orders of magnitude higher than what is achievable with conventional thin-film passivation layers. Notably, Nafion passivates the c-Si surface only by the fixed charges without chemical modification of dangling bonds, which is fundamentally different from the common practice of combining chemical with field-effect passivation. This dip coating process is simple and robust, without the need for complex equipment or parameter optimization as there is no chemical reaction involved.

Surface passivation of semiconductors is widely used to enhance the performance of photovoltaic and optoelectronic devices.^{1, 2} Attaining high effective carrier lifetimes (τ_{eff}) directly enables high implied open circuit voltages in silicon solar cells. As an indirect bandgap semiconductor, crystalline silicon (c-Si) possesses a long intrinsic carrier lifetime attributed to slow radiative and Auger recombination which can even reach a hundred milliseconds in lightly doped silicon.³ However, severe trap-assisted

recombination, generally known as Shockley-Read-Hall (SRH) recombination, typically leads to much shorter experimentally measured τ_{eff} . Despite significant bulk SRH suppression in high-quality float zone (FZ) c-Si, τ_{eff} is critically limited by surface SRH processes from large amounts of defect at its unpassivated surface.⁴ Chemical and field-effect passivation are commonly two effective ways to suppress surface SRH recombination. Chemical passivation methods often involve reactive species such as concentrated hydrofluoric acid (HF), iodine / methanol and hydrogenated amorphous silicon (a-Si:H), and thus reduce the interfacial defect density on the silicon surface to reach a low surface recombination velocity (SRV).⁵⁻⁸ Field-effect passivation can hinder the recombination at the interface by growing or depositing oxide and nitride thin films with fixed charges, e.g. SiN_x , AlO_x , SiO_x , TiO_x , ZrO_x , to induce band bending that results in asymmetric carrier concentrations.⁹⁻¹⁴ However, since the fixed charge density is generally not sufficiently high, state-of-the-art thin-film passivation almost always requires additional chemical passivation process such as post annealing, often in forming gas.

Ideally, the passivation processes should be non-destructible, stable and carried out at room temperature. Solution methods, e.g. concentrated HF, can be performed at room temperature whereas the passivated wafers have to be measured *in situ* due to the poor resilience to air exposure. The toxic and corrosive nature of HF also restricts its extensive use. Conversely, conventional thin-film passivation is more stable, but the deposition and post

annealing processes require moderate to high temperatures (200–1000 °C) which could alter the bulk lifetime by activating / deactivating metastable bulk defects.^{15,16} Additionally, the deposition processes are often complex and suffer from process variability, and utilize capital intensive equipment.⁹¹⁰ Thus, the development of passivation schemes that overcome the challenges above is of utmost interest for both bulk wafer metrology and high efficiency solar cells.

Organic materials for c-Si passivation have been studied from decades ago, but relatively high SRV and/or poor air-exposed longevity for *ex situ* characterization limited their wider application.^{5, 15, 16} Recently, several solution-processed thin-film passivation methods based on organic materials are emerging, including bis(trifluoromethane)sulfonimide (TFSI), polystyrene sulfonate and Nafion.¹⁷⁻¹⁹ However, their passivation mechanism still needs further exploration.

Herein, we report a dip coating method using the commercial polymer Nafion to attain near ideal surface passivation of c-Si wafers. Nafion is well-known for its strong Lewis acidity and has been used as effective heterogenous Lewis acid catalyst for reactions, including Friedel-Crafts alkylation and Diels-Alder reaction.^{20, 21} Due to the stable fluoropolymer matrix and immobilized sulfonic acid groups, Nafion is non-reactive and has been used in implantable sensors.^{22, 23} Our study demonstrates that Nafion dip coating provides c-Si surface passivation of up to $\tau_{\text{eff}} = 12$ ms. This simple and robust passivation method can be performed in ambient air and room

temperature, and is sufficiently stable to allow for subsequent surface characterization. From detailed experiments and simulations, Nafion passivation mechanism is attributed to interfacial charge transfer caused by Lewis acid-base interaction with the silicon surface, rather than chemically saturating surface silicon bonds. Notably, the lack of chemical reaction in this surface passivation scheme provides high reproducibility without the need for complex equipment or process parameter optimization, presenting a major advantage over the conventional techniques.

RESULTS AND DISCUSSION

The schematic illustration of our passivation procedure is shown in Figure 1a. Following a quick immersion in 5% vol. diluted HF solution for native oxide removal, (100) oriented mirror-polished c-Si wafers were dipped into the polymer solutions for 30 s. The remnant solvent was dried by nitrogen to yield polymer thin films. Subsequently, samples were characterized by photoconductance decay (PCD) method to extract τ_{eff} . The dip coating method coats both sides of the wafer with Nafion simultaneously and avoids chuck marks from spin coating resulting in unpassivated region on the surface which can reduce the measured lifetime. Four polymers, Nafion, poly(4-styrenesulfonic acid) (PSS), poly(acrylic acid) (PAA), and poly(methyl acetate) (PMMA) were evaluated for their passivation effects (Figure 1b). The passivation performance of these four polymers are shown in Figure 1c. Among these polymers, Nafion is the strongest Lewis acid and gives the

highest τ_{eff} of 12 ms, with a corresponding upper limit SRV of 2.6 cm s⁻¹ and emitter saturation current (j_0) of 16 fA cm⁻² (Figure S1).²⁴ This result is comparable with state-of-the-art thin-film passivation.^{10, 13, 14, 25} The passivation quality of c-Si wafers coated by PSS, PAA and PMMA is lower, with the τ_{eff} values of 2.5 ms, 0.1 ms and 0.03 ms respectively. As elucidated later, the observed passivation quality of the various polymers is consistent with their corresponding Lewis acidity. These results discussed above are measured on high resistivity FZ *n*-Si wafers with a doping concentration of 3.8×10^{13} cm⁻³ and at the injection level of 10^{15} cm⁻³.

The passivation effect of Nafion was then investigated on c-Si wafers of various doping types and concentrations, shown in Figure 2a. The results demonstrate Nafion thin films can passivate various c-Si surfaces. As expected, τ_{eff} decreases with the increase of doping concentration and τ_{eff} of *n*-Si is higher than that of *p*-Si, which is indeed consistent with bulk lifetime difference of various c-Si wafers. Samples coated by Nafion thin films have two orders of magnitude enhancement of τ_{eff} , compared to control samples with diluted HF dip only (Figure S2). This passivation effect is reversible and τ_{eff} drops back to less than 0.01 ms after Nafion removal by *i*-propanol. Notably, Nafion can be completely removed from the surface as evident from atomic force microscopy (AFM, Figure S3), thus the process can in principle be used as a non-destructive in-line metrology technique.

Nafion passivation is sufficiently air-stable to allow for various surface characterizations. When exposed to air, samples passivated by Nafion exhibit

better τ_{eff} stability than that of HF treated samples. The τ_{eff} of the Nafion passivated wafers reduces by approximately 30-40% after one-hour air exposure (Figure 2b) whereas τ_{eff} of HF treated samples drops two orders of magnitude in several minutes.¹⁷ We attribute this decrease of τ_{eff} for Nafion coated samples to a slow silicon surface oxidation process with residual oxygen and water molecules. It should be noted that Nafion is not reactive towards SiO_x and does not etch the native oxide.²⁶ As shown in a control experiment (Figure S4), wafers without native oxide removal (*i.e.*, without HF dip) could also be passivated by Nafion, although with a lower τ_{eff} of 1.5 ms. While wafers with and without HF dip show different τ_{eff} at the beginning, eventually both wafers reach similar τ_{eff} after prolonged air-exposure.

The c-Si orientation dependence of Nafion passivation was also explored. To ensure the same bulk quality, polished (100) *p*-type c-Si wafers were random pyramid-textured to expose (111) facets. The polished and textured c-Si wafers were passivated by Nafion. The two wafers showed negligible variation in the measured lifetime despite the differences in surface orientation and surface area. Since surface chemical reactions are known to have strong orientation dependence,²⁷ these results further depict that the Nafion does not modify the dangling bonds as part of the passivation. In distinct contrast, the same polished and textured wafers passivated with conventional *i/p* a-Si:H layers exhibit a 3x difference in τ_{eff} arising from different surface orientations (Figure S5a).

A strong evidence of charge transfer across Nafion / silicon interface was observed by electrical measurements of a back-gated ultrathin body (10 nm thick) silicon field-effect transistor with an open front side. After Nafion coating, a positive shift of 4V in the threshold voltage (V_{th}) was observed (Figure S5b), corresponding to negative charges in Nafion caused by interfacial charge transfer. This charge transfer is suppressed by the formation of silicon oxide at Nafion / silicon interface. Indeed, as described previously, the Nafion coated samples with native oxide exhibit a lower lifetime as compared to those with the oxide removed (Figure S4). Even more, control samples with thicker thermally grown SiO_2 yield non-measurable lifetime, which indicates oxide layers act as barriers to charge transfer.

Next, we model the effect of interfacial charge transfer on lifetime. The charge transfer occurring at the polymer / silicon interface results in the formation of fixed charges with a density Q_f . Lewis acid strength of the polymers and the surface density of their functional groups determine Q_f . As discussed later in detail, we estimate the upper limit $Q_f = 7 \times 10^{13} \text{ cm}^{-2}$ for Nafion. This Q_f value for Nafion is significantly higher than that of conventional thin-film passivation layers such as SiN_x ($10^{11} - 10^{12} \text{ cm}^{-2}$) and AlO_x ($10^{12} - 10^{13} \text{ cm}^{-2}$).^{3, 10, 28} SRV was calculated as a function of interface trap density (D_{it}) and Q_f (Figure S6).²⁹ Briefly, following the principle of charge neutrality at the interface, band bending is determined and the SRV is calculated. In order to convert SRV to τ_{eff} , the bulk lifetime was set to 47 ms.⁴

A contour plot of the calculated τ_{eff} is shown in Figure 3a, in which the dashed vertical line marks the upper limit Q_f of Nafion. Surprisingly, the dashed line depicts τ_{eff} of Nafion passivated surface is not affected by the interface traps over the calculated range of $D_{\text{it}}=10^8$ (minimal surface dangling bonds) to $10^{14} \text{ cm}^{-2} \text{ eV}^{-1}$ (nearly saturated with dangling bonds), and approaches the bulk lifetime value. This is consistent with the experimental observation that repairing the surface dangling bonds is not necessary for Nafion passivation. The passivation mechanism is illustrated by the calculated energy band diagrams in Figure 3b. Here we use $D_{\text{it}}=10^{12} \text{ cm}^{-2} \text{ eV}^{-1}$ which is the value reported in literature for the silicon surface after diluted HF treatment and calculated from control samples in Figure S2.³⁰ The band bending at the silicon surface is small before Nafion passivation when a practically minimum $Q_f = 10^8 \text{ cm}^{-2}$ is used for the calculation. In this case, electrons and holes easily recombine at the surface under illumination, resulting in a small τ_{eff} . On the other hand, large surface band bending is induced after Nafion coating ($Q_f = 7 \times 10^{13} \text{ cm}^{-2}$). Consequently, the minority carriers are repelled from the surface by the created electric field thus suppressing the surface recombination and leading to a high τ_{eff} .

We further studied the correlation between τ_{eff} and Lewis acidity. We used Nafion solutions partially neutralized to various degrees by a weak Lewis base, N,N'-dimethylaniline. Figure 4a shows the measured τ_{eff} as a function of neutralization, which is defined as molarity of added base divided by molarity of acid functional groups in Nafion. In this case, Nafion withdraws

electrons from N,N'-dimethylaniline rather than silicon with increasing neutralization. As expected, τ_{eff} decreases as the neutralization of Nafion increases.

Next, we studied the quality of surface passivation as a function of Lewis acidity by using different polymers. We choose pK_a as a simple guideline to define Lewis acidity of the polymers. Figure 4b shows the calculated Q_f as a function of pK_a for Nafion, PAA, PSS and PMMA. For simplicity, we assume that the amount of Lewis acid active sites is proportional to the amount of dissociated acid groups and one electron transfers at each active site. Then the upper limit of Q_f can be estimated by supposing the polymer chain is close packed on the silicon surface (acidic groups density from 0.5 to 10 nm^{-2} in this model). In Figure 4b, the light grey region represents the estimated upper limit Q_f that polymeric acids can reach. Colored circles show the upper limit Q_f for the four polymers. Here, pK_a can be regarded as an indicator of charge transfer efficiency at the polymer / silicon interface. As pK_a is reduced, Q_f increases. At sufficiently low pK_a (e.g. less than 0), the efficiency starts to approach unity; in this region Q_f saturates and does not further increase with lowering of pK_a . The calculated values are based on simple assumptions; actual Q_f may be slightly different due to uncertainty in charge transfer efficiency and surface coverage ratio. In the future, density functional theory can be used to more accurately estimate Q_f for different polymers. We also plot the measured and calculated τ_{eff} as a function of pK_a (Figure 4c). As expected, the calculated τ_{eff} follows the trend of Q_f as a

function of pK_a . The calculated τ_{eff} is consistent with the experimental results obtained for the four polymers, further validating the passivation mechanism.

Finally, other Lewis acid polymers with similar pK_a and sulfonic acid functional groups as with Nafion, such as 3M™ PFSA and Aquivion® are also effective in surface passivation (Figure S7), indicating the generality of the concept. And previous work of TFSI can also be attributed to this charge transfer effect.¹⁷ Similarly, Lewis bases show passivation effects as well. In this case, the Lewis base donates electrons to the silicon, resulting in positive fixed charges at the surface. Passivation performance of several weak and moderate Lewis bases are shown in Figure S8, which qualitatively follows the same trend as that of Lewis acid treatment. However, most strong Lewis bases are unstable or chemically react with silicon, thus are not explored in this study.

CONCLUSION

In this study, we have demonstrated a simple, dip coating passivation at room temperature by Nafion and other polymeric Lewis acids. The champion lifetime shows 12 ms on lightly doped FZ *n*-Si with significantly higher air-exposed longevity compared to conventional solution treatments. Its simplicity and effectiveness make Nafion passivation a powerful, fab-friendly method for lifetime metrology. The mechanism of Nafion passivation is attributed to charge transfer at the Nafion / silicon interface, resulting in high

density of surface fixed charges and strong surface band bending. Simulations and experiments demonstrate the feasibility of near-ideal passivation without modifying silicon dangling bonds. As a result, the process is simple and robust, with minimal process variability. In the future, this passivation concept can be extended to the use of *inorganic* Lewis acids / bases which represent a diverse and tunable chemical library within which other materials for stable surface and contact passivation may be discovered. Finally, the concept should also be applicable to other semiconductors, and could have broader scientific and practical impact beyond silicon solar cells. For example, our preliminary findings show that Nafion also serves as an ideal passivation layer for monolayer semiconductors (Figure S9).

METHODS

Passivation of c-Si

The polymer acids, Nafion[®] perfluorinated resin solution (5 wt.% in lower aliphatic alcohols and water, contains 15–20% water), Aquivion[®] D83-06A dispersion (6% PFSA in lower aliphatic alcohols and water, water 20%), poly(4-styrenesulfonic acid) solution ($M_w \sim 75,000$, 18 wt.% in H₂O) and poly(acrylic acid) solution (average $M_w \sim 100,000$, 35 wt.% in H₂O) were purchased from Sigma-Aldrich. 3M[™] PFSA 800EW powder were provided by 3M Company and dissolved as 5 wt.% in the solution of ethanol: *i*-propanol: water = 4:2:1. Nafion[®], Aquivion[®] and 3M[™] solutions were diluted to 1 wt.%

by ethanol. To keep a constant acid molarity, poly(4-styrenesulfonic acid) and poly(acrylic acid) were diluted to 0.2 wt.% and 0.1 wt.% by ethanol respectively. PMMA C2 was purchased from MicroChem Corporation. Samples for lifetime measurements are prepared using (100), FZ, *n*-type ($5 \times 10^{15} \text{ cm}^{-3}$, $4 \times 10^{13} \text{ cm}^{-3}$) and *p*-type ($1 \times 10^{16} \text{ cm}^{-3}$, $2 \times 10^{15} \text{ cm}^{-3}$) c-Si wafers. Before polymers coating, samples were subjected to a dilute HF (5% vol.) dip to remove native oxide. Subsequently, tested wafers were dipped in polymer solutions (~30 s) followed by N₂ blow dry. All the aforementioned processes were operated in ambient air. PCD measurements were conducted using a Sinton WCT 120 photoconductance tester in the transient mode. In the experiments of orientation dependence, polished wafers with a doping concentration of $4.9 \times 10^{15} \text{ cm}^{-3}$ were tested. Textured wafers were chemically etched in a solution of dilute KOH from the same batch of polished wafers. On these reference samples, a stack of intrinsic and boron-doped amorphous silicon was deposited *via* PECVD in an INDEOtec Octopus II reactor at 200 °C after standard RCA cleaning and dipping in a dilute HF solution. AFM for Nafion removal measurements was conducted by a Dimension ICON AFM (Bruker, Germany) under ambient conditions.

Device Fabrication and Characterization

Back-gated ultrathin body silicon field-effect transistors were fabricated on a (100) SOI 200mm wafer with 12-nm-thick top silicon, 25-nm-thick buried oxide and 500- μm -thick silicon handle wafer. Top silicon and handle wafer silicon were both lightly doped by boron (*p*), with a starting resistivity of 10

to $30 \Omega \text{ cm}$ ($0.45\text{--}1 \times 10^{15} \text{ cm}^{-3}$). Source and drain were then phosphorus doped with the concentration of $1 \times 10^{20} \text{ cm}^{-3}$. After that, 20 nm Ni and 50 nm W were sputtered as source / drain contacts. A following forming gas annealing at $350 \text{ }^\circ\text{C}$ for 5 min was processed for contact silicidation. 1 wt.% Nafion solution was dropped on front open side. Transistor $I_D\text{--}V_G$ characteristics of tested devices were taken using an Agilent 4155C semiconductor parameter analyzer.

Photoluminescence (PL) Measurement

MoS_2 and WS_2 monolayers were mechanically exfoliated on SiO_2/Si substrates and identified by optical contrast and AFM. 5 wt.% Nafion solution was dropped on tested monolayers and blown dry by N_2 . The PL quantum yield was measured by a customized micro-PL instrument which is described in detail in previous studies.^{31, 32} An Ar ion laser with a 514.5 nm line was utilized as the excitation source. All the PL measurements were performed at room temperature and in an ambient lab environment.

Simulations

Calculated τ_{eff} vs. interface trap and fixed charge densities adopted the model by Girisch *et al.*²⁹ Following parameters are used for simulation: $N(n)=3.8 \times 10^{13} \text{ cm}^{-3}$, $\epsilon_{\text{Si}}=11.68 \epsilon_0$, $\sigma_n=3 \times 10^{-16} \text{ cm}^2$, $\sigma_p=10^{-16} \text{ cm}^2$, thickness $t=625 \mu\text{m}$ and injection level $\Delta n=1 \times 10^{15} \text{ cm}^{-3}$. The τ_{eff} vs. pK_a curve in Fig. 4c was calculated with the assumption of $D_{\text{it}}=10^{12} \text{ cm}^{-2} \text{ eV}^{-1}$.

Calculation of Q_f vs. pK_a was based on principles and estimations from textbooks and handbooks. Two assumptions were made: 1) all the polymers

are closed-packed on the surface as an ideal crystallization and 2) the amount of Lewis acid active sites is proportional to the amount of dissociated acid groups. Since one acidic group is in one monomer for tested polymer acids, the coverage density based on assumption 1 is determined by the size of monomers S which can be roughly estimated by chemical bonds lengths and van der Waals radius. Assumption 2 was further defined that one electron transferred at each active site to simplify the case. The amount of dissociated acid groups n were calculated by following equation:

$$n = \frac{\alpha}{S}$$

In which

$$\alpha = \frac{-K_a + \sqrt{K_a^2 + 4K_a C}}{2C}, \quad C = \frac{\rho}{EW}$$

where α is dissociation degree, ρ and EW are the density and equivalent weight of specific polymers.

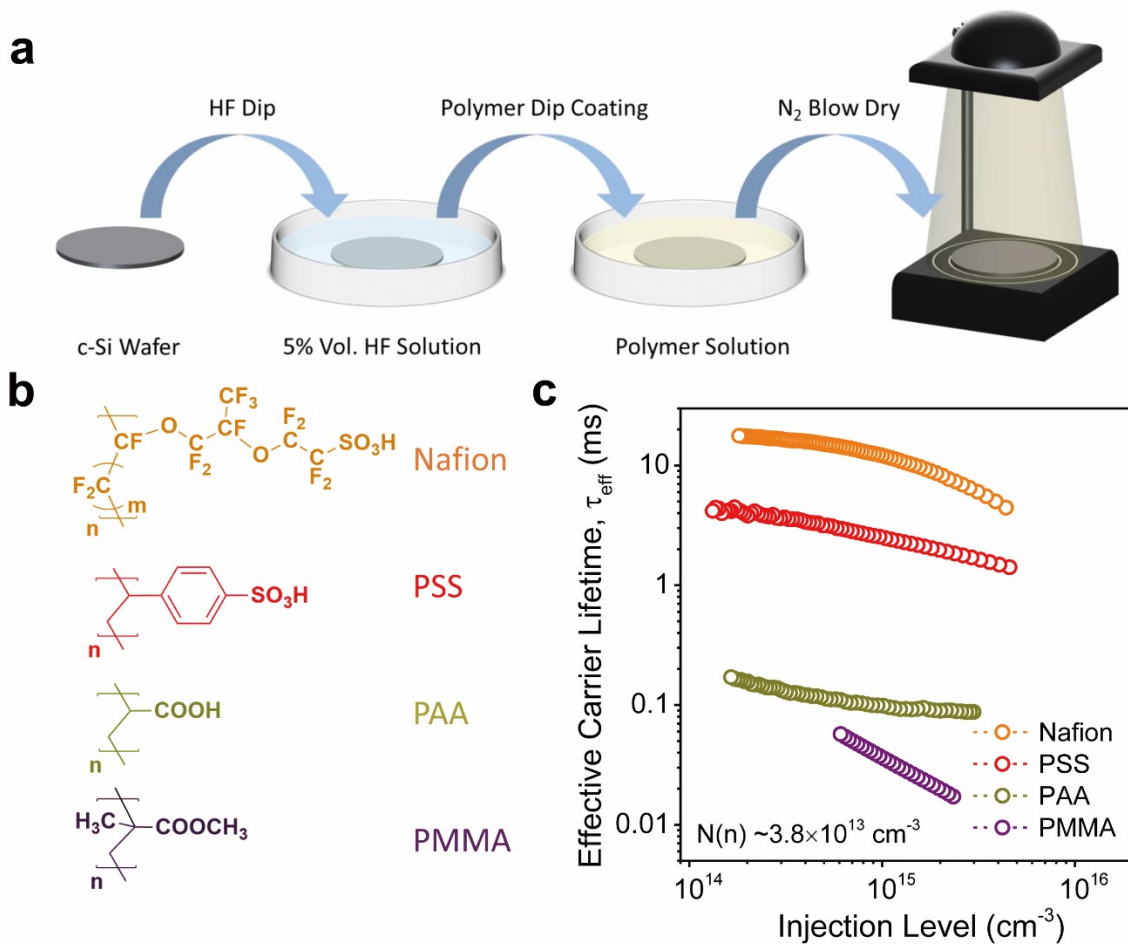


Figure 1. (a) Schematic illustration of the passivation procedure. (b) Chemical structures of four different polymers used in this study. (c) τ_{eff} vs. injection level measured on lightly doped ($3.8 \times 10^{13} \text{ cm}^{-3}$) *n*-type c-Si wafers passivated by the four polymers.

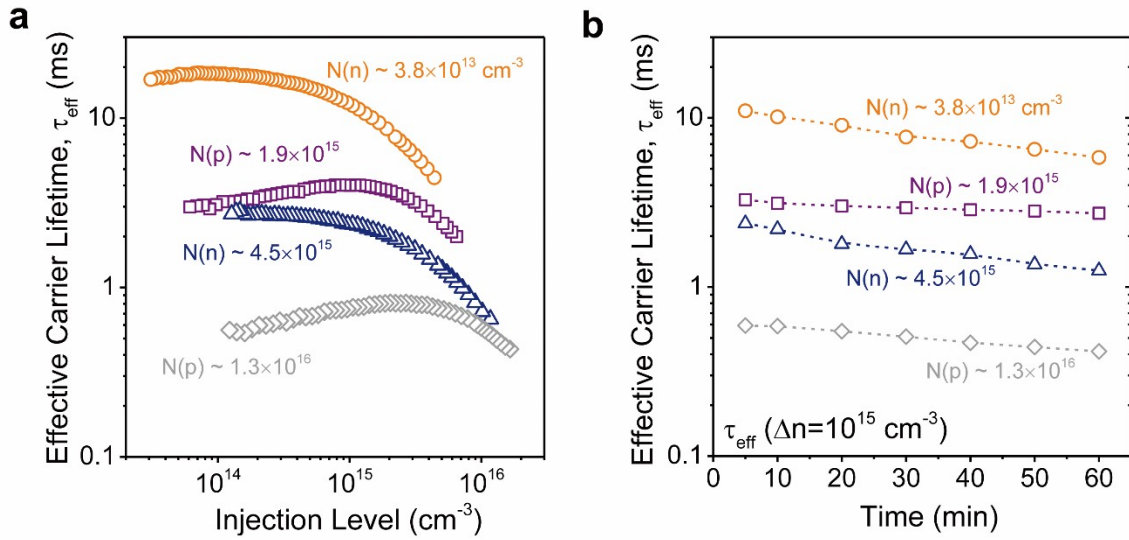


Figure 2. (a) τ_{eff} vs. injection level, and (b) air-exposed stability for Nafion coated c-Si wafers with four different doping types and concentrations. Doping concentrations of *n*- and *p*-type wafers are labelled as $N(n)$ and $N(p)$, respectively.

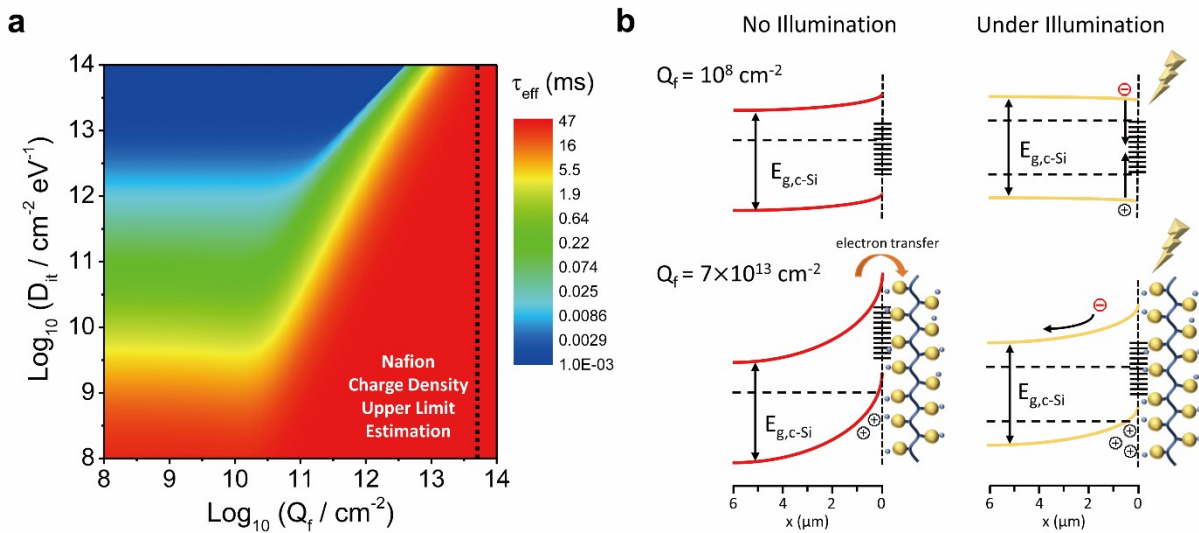


Figure 3. (a) Contour plot of calculated τ_{eff} vs. interface trap density and fixed charge density, in which 47 ms is assumed as the bulk lifetime of wafers for simulation. The dash line depicts the expected lifetime values for Nafion passivation assuming $Q_f = 7 \times 10^{13} \text{ cm}^{-2}$. (b) Calculated energy band diagrams of silicon surface with (bottom two panels) and without (top two panels) Nafion passivation in dark (left panels) and under illumination (right panels).

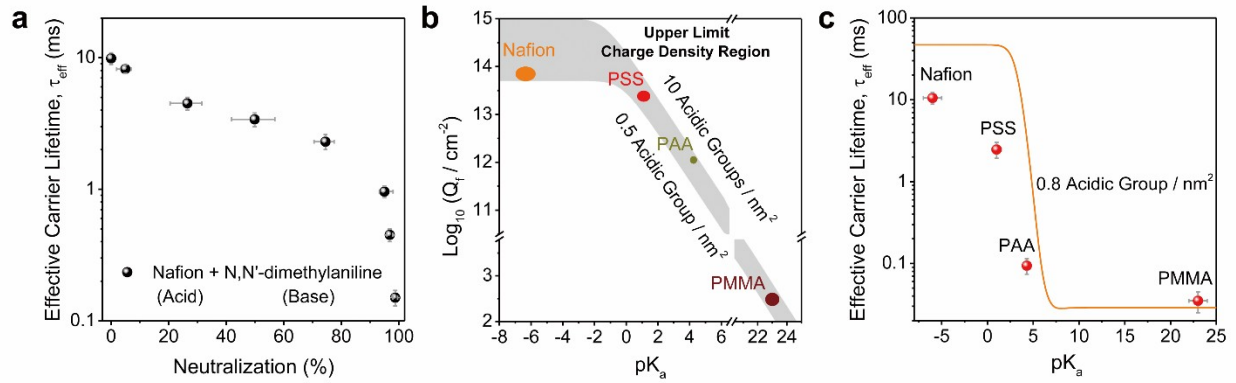
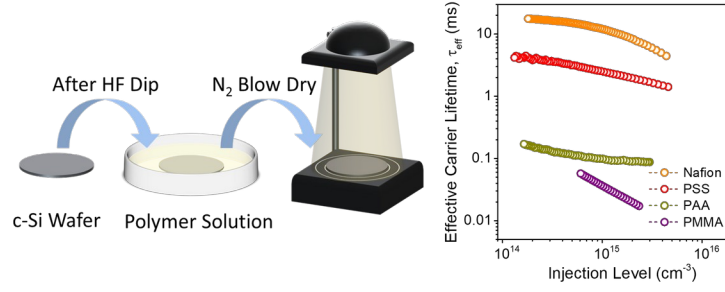


Figure 4. (a) Measured τ_{eff} of Nafion passivation of various degrees of neutralization by Lewis base N,N'-dimethylaniline. (b) Calculated fixed charge density vs. pK_a in which the upper limit Q_f of four polymers are circled by different colors. (c) Calculated τ_{eff} as a function of pK_a (orange line). The measured τ_{eff} for the four polymers are also shown (pink dots). The error bars depict the variation in literature reported pK_a and in lifetime measurements. All the results are measured on lightly doped ($3.8 \times 10^{13} \text{ cm}^{-3}$) *n*-type c-Si wafers at the injection level of 10^{15} cm^{-3} .

TOC Graphic



ASSOCIATED CONTENT

The authors declare no competing financial interests.

Supporting Information

The Supporting Information is available free of charge on the ACS Publications website.

Extracted emitter saturation current (J_0) of Nafion passivated wafer. Control experiments of Nafion passivation. The removal of Nafion passivation layers. Nafion passivation on c-Si wafers with native oxide. Experiments for passivation mechanism of Nafion. SRV simulations used to create Figure 3a. Passivation performances of perfluorinated sulfonic acid (PFSA). Lewis bases passivation performance. Nafion passivation for transition metal dichalcogenides.

AUTHOR INFORMATION

Corresponding Author

*E-mail: ajavey@berkeley.edu

ORCID

Wenbo Ji: 0000-0002-7913-361X

Yingbo Zhao: 0000-0002-6289-7015

Der-Hsien Lien: 0000-0001-6774-2074

Ali Javey: 0000-0001-7214-7931

Author Contributions

W.J., Y.Z. and A.J. conceived the idea. W.J. carried out the passivation measurements, electrical characterization, simulations and analysis. Y.Z.

discussed the results and assisted with simulations. H.M.F. fabricated devices and assisted with electrical characterization. J.B. and T.G.A. discussed the results and assisted with passivation measurements. D.-H.L. assisted with PL measurements. S.D.W. discussed the results. W.J. wrote the paper and all other authors provided feedback.

ACKNOWLEDGMENT

We would like to thank Scott Bentrup of 3M Company for providing 3M™ PFSA powders for passivation test. Passivation characterization and concept development were supported by the Electronic Materials Programs, funded by the Director, Office of Science, Office of Basic Energy Sciences, Material Sciences and Engineering Division of the U.S. Department of Energy under Contract No. DE-AC02-05CH11231. Device fabrication was funded by U.S. Department of Energy, Solar Energy Technologies Office under the Contract No. DE-EE0008162 and King Abdullah University of Science & Technology under the Contract No. OSR-2017-GRGG-3383.01.

REFERENCES

1. Aberle, A. G., Surface Passivation of Crystalline Silicon Solar Cells: a Review. *Prog. Photovolt: Res. Appl.* **2000**, *8*, 473-487.
2. Schnitzer, I.; Yablonovitch, E.; Caneau, C.; Gmitter, T.; Scherer, A., 30% External Quantum Efficiency from Surface Textured, Thin-Film Light-Emitting Diodes. *Appl. Phys. Lett.* **1993**, *63*, 2174-2176.

3. Cuevas, A.; Allen, T.; Bullock, J.; Wan, Y.; Zhang, X. Skin Care for Healthy Silicon Solar Cells. In *2015 IEEE 42nd Photovoltaic Specialist Conference (PVSC)*; June 14–19, 2015; New Orleans, LA, USA; pp 1-6.
4. Richter, A.; Glunz, S. W.; Werner, F.; Schmidt, J.; Cuevas, A., Improved Quantitative Description of Auger Recombination in Crystalline Silicon. *Phys. Rev. B* **2012**, *86*, 165202.
5. Yablonovitch, E.; Allara, D.; Chang, C.; Gmitter, T.; Bright, T., Unusually Low Surface-Recombination Velocity on Silicon and Germanium Surfaces. *Phys. Rev. Lett.* **1986**, *57*, 249.
6. Grant, N. E.; McIntosh, K. R.; Tan, J.; Rougieux, F.; Bullock, J.; Wan, Y.; Barugkin, C. Light Enhanced Hydrofluoric Acid Passivation for Evaluating Silicon Bulk Lifetimes. In *28th European Photovoltaic Solar Energy Conference and Exhibition (EU PVSEC)*; Oct 1–3, 2013; Paris, France; pp 883-887.
7. M'saad, H.; Michel, J.; Lappe, J.; Kimerling, L., Electronic Passivation of Silicon Surfaces by Halogens. *J. Electron. Mater.* **1994**, *23*, 487-491.
8. De Wolf, S.; Beaucarne, G., Surface Passivation Properties of Boron-Doped Plasma-Enhanced Chemical Vapor Deposited Hydrogenated Amorphous Silicon Films on *P*-Type Crystalline Si Substrates. *Appl. Phys. Lett.* **2006**, *88*, 022104.
9. Lauinger, T.; Schmidt, J.; Aberle, A. G.; Hezel, R., Record Low Surface Recombination Velocities on 1 Ω cm *P*-Silicon Using Remote Plasma Silicon Nitride Passivation. *Appl. Phys. Lett.* **1996**, *68*, 1232-1234.
10. Agostinelli, G.; Delabie, A.; Vitanov, P.; Alexieva, Z.; Dekkers, H.; De Wolf, S.; Beaucarne, G., Very Low Surface Recombination Velocities on *P*-Type Silicon Wafers Passivated With a Dielectric With Fixed Negative Charge. *Sol. Energy Mater. Sol. Cells* **2006**, *90*, 3438-3443.
11. Hoex, B.; Schmidt, J.; Bock, R.; Altermatt, P.; Van De Sanden, M.; Kessels, W., Excellent Passivation of Highly Doped *P*-Type Si Surfaces by the Negative-Charge-Dielectric Al₂O₃. *Appl. Phys. Lett.* **2007**, *91*, 112107.
12. Aberle, A.; Glunz, S.; Stephens, A.; Green, M., High-Efficiency Silicon Solar Cells: Si/SiO₂, Interface Parameters and Their Impact on Device Performance. *Prog. Photovolt: Res. Appl.* **1994**, *2*, 265-273.
13. Liao, B.; Hoex, B.; Aberle, A. G.; Chi, D.; Bhatia, C. S., Excellent c-Si Surface Passivation by Low-Temperature Atomic Layer Deposited Titanium Oxide. *Appl. Phys. Lett.* **2014**, *104*, 253903.
14. Wan, Y.; Bullock, J.; Hettick, M.; Xu, Z.; Yan, D.; Peng, J.; Javey, A.; Cuevas, A., Zirconium Oxide Surface Passivation of Crystalline Silicon. *Appl. Phys. Lett.* **2018**, *112*, 201604.
15. Sieval, A. B.; Huisman, C. L.; Schönecker, A.; Schuurmans, F. M.; van der Heide, A. S.; Goossens, A.; Sinke, W. C.; Zuilhof, H.; Sudhölter, E. J., Silicon Surface Passivation by Organic Monolayers: Minority Charge Carrier Lifetime Measurements and Kelvin Probe Investigations. *J. Phys. Chem. B* **2003**, *107*, 6846-6852.
16. Biro, D.; Warta, W., Low Temperature Passivation of Silicon Surfaces by Polymer Films. *Sol. Energy Mater. Sol. Cells* **2002**, *71*, 369-374.

17. Bullock, J.; Kiriya, D.; Grant, N.; Azcatl, A.; Hettick, M.; Kho, T.; Phang, P.; Sio, H. C.; Yan, D.; Macdonald, D.; Quevedo-Lopez, M. A.; Wallace, R. M.; Cuevas, A.; Javey, A., Superacid Passivation of Crystalline Silicon Surfaces. *ACS Appl. Mater. Interfaces* **2016**, *8*, 24205-24211.
18. Schmidt, J.; Titova, V.; Zielke, D., Organic-Silicon Heterojunction Solar Cells: Open-Circuit Voltage Potential and Stability. *Appl. Phys. Lett.* **2013**, *103*, 183901.
19. Chen, J.; Ge, K.; Zhang, C.; Guo, J.; Yang, L.; Song, D.; Li, F.; Xu, Z.; Xu, Y.; Mai, Y., Vacuum-Free, Room-Temperature Organic Passivation of Silicon: Toward Very Low Recombination of Micro-/Nanotextured Surface Structures. *ACS Appl. Mater. Interfaces* **2018**, *10*, 44890-44896.
20. Olah, G. A.; Kaspi, J.; Bukala, J., Heterogeneous Catalysis by Solid Superacids. 3. Alkylation of Benzene and Transalkylation of Alkylbenzenes Over Graphite-Intercalated Lewis Acid Halide and Perfluorinated Resin Sulfonic Acid (Nafion-H) Catalysts. *J. Org. Chem.* **1977**, *42*, 4187-4191.
21. Olah, G. A.; Meidar, D.; Fung, A. P., Synthetic Methods and Reactions; 59. Catalysis of Diels-Alder Reactions by Nafion-H Perfluorinated Resinsulfonic Acid. *Synthesis* **1979**, *1979*, 270-271.
22. Turner, R. F.; Harrison, D. J.; Rojotte, R. V., Preliminary *in Vivo* Biocompatibility Studies on Perfluorosulphonic Acid Polymer Membranes for Biosensor Applications. *Biomaterials* **1991**, *12*, 361-368.
23. Lu, J.; Do, I.; Drzal, L. T.; Worden, R. M.; Lee, I., Nanometal-Decorated Exfoliated Graphite Nanoplatelet Based Glucose Biosensors With High Sensitivity and Fast Response. *ACS Nano* **2008**, *2*, 1825-1832.
24. Sproul, A., Dimensionless Solution of the Equation Describing the Effect of Surface Recombination on Carrier Decay in Semiconductors. *J. Appl. Phys.* **1994**, *76*, 2851-2854.
25. Allen, T.; Cuevas, A., Electronic Passivation of Silicon Surfaces by Thin Films of Atomic Layer Deposited Gallium Oxide. *Appl. Phys. Lett.* **2014**, *105*, 031601.
26. Harmer, M. A.; Farneth, W. E.; Sun, Q., High Surface Area Nafion Resin/Silica Nanocomposites: a New Class of Solid Acid Catalyst. *J. Am. Chem. Soc.* **1996**, *118*, 7708-7715.
27. Stathis, J.; Dori, L., Fundamental Chemical Differences Among P_b Defects on (111) and (100) Silicon. *Appl. Phys. Lett.* **1991**, *58*, 1641-1643.
28. Schmidt, J.; Aberle, A. G., Carrier Recombination at Silicon-Silicon Nitride Interfaces Fabricated by Plasma-Enhanced Chemical Vapor Deposition. *J. Appl. Phys.* **1999**, *85*, 3626-3633.
29. Girisch, R. B.; Mertens, R. P.; De Keersmaecker, R., Determination of Si-SiO₂ Interface Recombination Parameters Using a Gate-Controlled Point-Junction Diode Under Illumination. *IEEE Trans. Electron Devices* **1988**, *35*, 203-222.
30. Angermann, H.; Wolke, K.; Gottschalk, C.; Moldovan, A.; Roczen, M.; Fittkau, J.; Zimmer, M.; Rentsch, J., Electronic Interface Properties of Silicon Substrates after Ozone Based Wet-Chemical Oxidation Studied by SPV Measurements. *Appl. Surf. Sci.* **2012**, *258*, 8387-8396.

31. Amani, M.; Lien, D.-H.; Kiriya, D.; Xiao, J.; Azcatl, A.; Noh, J.; Madhvapathy, S. R.; Addou, R.; Santosh, K.; Dubey, M., Near-Unity Photoluminescence Quantum Yield in MoS₂. *Science* **2015**, *350*, 1065-1068.
32. Amani, M.; Taheri, P.; Addou, R.; Ahn, G. H.; Kiriya, D.; Lien, D.-H.; Ager III, J. W.; Wallace, R. M.; Javey, A., Recombination Kinetics and Effects of Superacid Treatment in Sulfur-and Selenium-Based Transition Metal Dichalcogenides. *Nano Lett.* **2016**, *16*, 2786-2791.